

Postcollision Interaction in the Coincident Emission of Photoelectrons and Auger Electrons at Small Relative Angles

N. Scherer, H. Lörch, T. Kerkau, and V. Schmidt

Fakultät für Physik, Universität Freiburg, D-79104 Freiburg, Germany

(Received 8 September 1998)

Postcollision interaction effects have been investigated for sequential two-electron emission in xenon for particular kinematical conditions, small relative angles between the emitted electrons, and selected energies $\epsilon_a = \epsilon_b$ which are halfway in between the nominal values of the “photo”-electron and the “Auger” electron. The experimental results are in good agreement with the theoretical prediction. Our successful technique to measure two coincident electrons of nearly the same energy and the same directions opens a plethora of possibilities to probe for different cases the Coulomb interaction of three charged particles and the impact of the intermediate resonance state. [S0031-9007(99)09343-6]

PACS numbers: 32.80.Hd

Since Newton it is known from celestial mechanics that a full solution for the motion of three bodies is hardly possible. This “three-body problem” is a fundamental one for all systems where three particles are linked by inverse square central forces. In particular, it also holds for the dynamics of three charged particles in the continuum which are subject to their mutual long-range Coulomb interactions. An important example for such a case is double photoionization, provided the emitted electrons, measured in coincidence, are analyzed with respect to their kinetic energies ϵ_a and ϵ_b and their directions \hat{k}_a and \hat{k}_b . Double photoionization can occur in two limiting forms, a direct one with the simultaneous emission of two photoelectrons, and an indirect one, usually called a “two-step” process, with the sequential emission of a photoelectron and an Auger electron. Here we concentrate on an indirect process characterized by the existence of a well-defined intermediate hole state. This introduces a time delay between the emitted electrons, and it leads to two interfering amplitudes. Since the degree of interference can be selected by the kinematical conditions set in the experiment and interference effects are known to provide a sensitive test to theoretical approaches, we deal with a system where many ways exist to explore in detail dynamical aspects of three-particle Coulomb interactions in sequential two-electron emission. In particular, we focus in the present work on cases where the emitted electrons have small relative angles and equal or nearly equal energies.

For the correct theoretical formulation of the sequential process the conventional two-step formulation must be replaced by a one-step formula [1], the antisymmetry of the final-state wave function leads to two amplitudes in the transition matrix element T_{fi} [2], and angle-dependent effects of postcollision interaction (PCI) play an important role [3]. One then gets an analytical expression for the nontrivial dependences on the emission angles (\hat{k}_a , \hat{k}_b) and the actual kinetic energies (ϵ_a , ϵ_b); the latter entering as differences to the nominal kinetic energies

$\epsilon_P^0 = h\nu - E_I^+$ and $\epsilon_A^0 = E_I^+ - E_I^{++}$ of the “photo”-electron and the “Auger” electron ($h\nu$ is the photon energy, E_I^+ and E_I^{++} the intermediate hole state and final state ionization energy, respectively). Depending on the energy settings selected in the experiment, one can explore rather distinct cases for such a sequential process. For $\epsilon_a = \epsilon_b$ the matrix element T_{fi} is governed by full coherence of both amplitudes. For ϵ_a very different from ϵ_b one has complete incoherence, i.e., only one of the two amplitudes in the transition matrix element T_{fi} is of relevance and the cross terms between the two amplitudes vanish (note that each of these amplitudes can be the dominant one, i.e., one gets two complementary transitions). Within these limits any ratio between the amplitudes is possible. A particular case can then be selected by the experimental conditions and will manifest in specific features in the angle- and energy-dependent coincidence signal between the emitted electrons. This tunability of coherence/incoherence provides a remarkable formal analogy with experiments in quantum optics in which the decoherence of a mesoscopic superposition of quantum states due to the coupling of the system to its environment is studied (see, e.g., [4]).

It is our aim to take full advantage of the experimental tuning possibilities to study PCI phenomena in different energy regions. Since the PCI mechanism relies on the three-body scattering wave function whose individual parts are grouped in a particular way (for details, see [5]), one gets a mutual interplay between the Coulomb repulsion between the ejected electrons (Sommerfeld factor) and an additional factor (resonance factor) which takes care of the intermediate state [3]. At full coherence and within an energy range ΔE_r dictated by Γ the sequential process becomes governed by the Sommerfeld factor (Γ is the level width of the intermediate state). This prohibits electron emission into the same direction and leads to an apparent analogy with direct double photoionization. However, at full incoherence and within ΔE_r the resonance factor dominates and for negligible

PCI effects, electron emission into the same direction occurs with equal probability as electron emission into the opposite direction.

The strongest PCI effects exist at small relative angles between the emitted electrons. Since here the “photo”-electron gains energy and the “Auger” electron loses the same amount (note, this is the opposite energy exchange as in noncoincident PCI), one gets for $\epsilon_P^0 < \epsilon_A^0$ a significant extension of ΔE_r which enhances interference effects as compared to $\Delta E_r \approx \Gamma$. This facilitates the experimental observation of PCI induced features which have been predicted theoretically [3], but not yet explored experimentally: a remarkable intensity for rather large energy detunings $\Delta E = \epsilon_P^0 - \epsilon_A^0 < 0$, accompanied by pronounced interference structures in the energy distribution of the coincident electrons, and a PCI induced reduction of the transition probability (see also [6]).

For our experimental study of PCI at small relative angles between the emitted electrons we selected $4d_{5/2}$ photoionization in xenon with subsequent $N_5-O_{2,3}O_{2,3}(^1S_0)$ Auger decay. For this case direct double photoionization is negligible, the nominal kinetic energies are $\epsilon_P^0 = h\nu - 67.55$ eV and $\epsilon_A^0 = 29.97$ eV, and the level width of the intermediate state is $\Gamma = 0.12$ eV.

In Fig. 1 we show examples for coincident energy distributions which we calculated by following the correct theoretical treatment described above. The photoionization matrix elements are from [7], the Auger decay matrix element with one partial wave only is set to unity. The data refer to completely linearly polarized incident light and observation of the emitted electrons in a plane defined by the directions of the photon beam and the electric field vector. Within this plane the acceptance angles Φ_a and Φ_b for the two coincident electrons are symmetric with respect to the electric field vector with values of $\Phi_a = +8^\circ$, $\Phi_b = -8^\circ$ (left part of the figure; relative angle $\Phi_{a,b} = 16^\circ$) and $\Phi_a = +12^\circ$, $\Phi_b = -12^\circ$ (right part of the figure; $\Phi_{a,b} = 24^\circ$). Further, the data are shown for different detuning parameters $\Delta E = \epsilon_P^0 - \epsilon_A^0$ (indicated in the figure). Pronounced PCI and interference effects can be seen for the “off-resonance” cases with $\Delta E < 0$ eV. One striking example is the additional structure at $\epsilon = (\epsilon_P^0 + \epsilon_A^0)/2$ in the spectrum with $\Delta E = -1$ eV and $\Phi_{a,b} = 16^\circ$, which clearly demonstrates that any association to a “photo”-electron and an “Auger” electron becomes meaningless here. “On-resonance” with $\Delta E = 0$ eV, and depending sensitively on the relative angle, a minimum or maximum occurs. For $\Delta E = +1$ eV the coincident energy distributions show two peaks close to the nominal values of ϵ_P^0 and ϵ_A^0 with strongly asymmetric shapes. Here the photoelectron simply gains energy and the Auger electron loses the same amount.

A direct measurement of coincident energy distributions like the ones shown in Fig. 1 poses extreme difficulties to any experimental setup, because two electrons of nearly the same energy and nearly the same direction must be measured in coincidence. If two separate electron spectrometers are used, their outside dimensions set a lower limit to the minimum angle of $\Phi_{a,b}$ (e.g., 45° in our experimental setup [8]). If a single electron spectrometer is used in conjunction with a single position sensitive detector, the limit is set by the multihit capability of the detector. To overcome this problem, we restrict our study in the present work to one particular aspect of these energy distributions: the photon energy dependence of coincident electrons with energies $\epsilon_a = \epsilon_b = (\epsilon_P^0 + \epsilon_A^0)/2$, i.e., we search under the full-coherence condition for PCI influences as manifested at point “A” in Fig. 1. The restriction to these energies opens access to study PCI phenomena at small relative angles by small modifications in our experimental setup.

The experiment was performed at the electron storage ring BESSY I in Berlin. We use only one electron spectrometer and equip it with two separate channeltron detectors mounted slightly outside the focal position (image of the pointlike source volume). Since the detected electrons have passed the same electric field of the analyzer their energies are equal and can be selected by the pass energy of the spectrometer, $\epsilon_a = \epsilon_b = E_{\text{pass}}$. Since the two

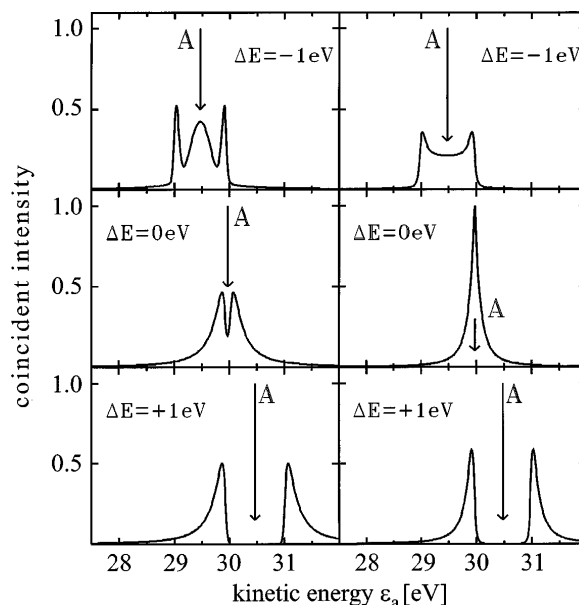


FIG. 1. Coincident energy distributions predicted theoretically for $4d_{5/2}$ photoionization and $N_5-O_{2,3}O_{2,3}(^1S_0)$ Auger decay in xenon. Shown are different relative angles (left column $\Phi_{a,b} = 16^\circ$, right column $\Phi_{a,b} = 24^\circ$) and different detuning parameters $\Delta E = \epsilon_P^0 - \epsilon_A^0$ as indicated. The energy scale is given for ϵ_a ; the energy ϵ_b of the coincident partner electron follows from energy conservation, $\epsilon_a + \epsilon_b = h\nu - E_{I^{++}}$. The point “A” indicates the special energies $\epsilon_a = \epsilon_b = (\epsilon_P^0 + \epsilon_A^0)/2$.

channeltrons are mounted outside the focal point, they accept electrons which are emitted at different angles. Ray-tracing calculation shows that each detector accepts a cone with an effective opening angle of $\Delta\Phi_a = \Delta\Phi_b = 2^\circ$ against its symmetry axis, set at the angles $\Phi_a = +10^\circ$, $\Phi_b = -10^\circ$ introduced above. Thus, our experimental setup allows the detection of coincident electrons at the selected energies (point “A”) within the angular range from $\Phi_{a,b} = 16^\circ$ to $\Phi_{a,b} = 24^\circ$ (compare Fig. 1)

The signal of observed coincidences contains several contributions which must be taken into account carefully. There are true coincidences of the desired process of $4d_{5/2}$ photoionization with subsequent $N_5\text{-O}_{2,3}\text{O}_{2,3}(^1S_0)$ Auger decay, abbreviated by $C_{\text{true}}(4d_{5/2})$. At higher photon energies one finds true coincidences of the related process of $4d_{3/2}$ photoionization with subsequent $N_4\text{-O}_{2,3}\text{O}_{2,3}(^1S_0)$ Auger decay, abbreviated by $C_{\text{true}}(4d_{3/2})$. In both cases one has random coincidences, C_{random} , which can be measured and subtracted easily by standard techniques. However, in addition there can exist coincidences C_{scat} which are produced if a primary electron scatters at a mesh at the spectrometer exit and produces a time-correlated secondary electron there, and each of these electrons gets detected in one of the two channeltrons. The contribution from C_{scat} was studied by measuring coincidences between $4d_{3/2}$ photoelectrons and $N_5\text{-O}_{2,3}\text{O}_{2,3}(^1S_0)$ Auger electrons, because there one can have only random coincidences and coincidences from the described scattering process. With an optimized field combination in front of the channeltrons we could suppress C_{scat} to practically zero (see open circles in Fig. 2 below).

Since PCI effects between $4d_{3/2}$ photoelectrons and $N_4\text{-O}_{2,3}\text{O}_{2,3}(^1S_0)$ Auger electrons extend into the energy region of $4d_{5/2}$ photoionization with subsequent $N_5\text{-O}_{2,3}\text{O}_{2,3}(^1S_0)$ Auger decay, both channels interfere. Consequently, the observed true coincidences will be termed $C_{\text{true}}(4d)$, but below 98 eV photon energy the data refer mainly to $C_{\text{true}}(4d_{5/2})$, and above this value mainly to $C_{\text{true}}(4d_{3/2})$.

Comparing the coincidence signal in Fig. 1 at point “A” for the detunings $\Delta E \leq 0$ one can see that the observed intensity depends critically on the actual angles accepted by the two channeltrons. These angles follow from the geometrical arrangement of the two channeltrons, with the exception that the effective cone angles $\Delta\Phi_a$ and $\Delta\Phi_b$ given above are by 30% smaller than their geometrical value. This reduction was determined from the measured shape of the noncoincident $N_5\text{-O}_{2,3}\text{O}_{2,3}(^1S_0)$ Auger line whose observed width must match the spectrometer resolution, since the latter depends on the size of the channeltron opening along the direction of energy dispersion. The reason for this reduction can be ascribed to a loss of detection efficiency at the border of the channeltron cone.

The experimental results of $C_{\text{true}}(4d)$ coincidences are shown in Fig. 2 as full points. The largest uncertainty

for the zero level of these true coincidences comes from C_{scat} which, however, is strongly suppressed. This can be seen from the measured C_{scat} values (open circles; compare above) as well as from an estimation (dotted curve) which is based on the relation $C_{\text{scat}} \approx 10^{-6} \times N$, found experimentally, where N is the sum of the single counting rates in both detectors. For comparison two theoretical predictions are plotted, the solid curve for PCI included, the dashed curve for PCI neglected. In both cases the experimental energy resolutions and the effects of finite acceptance angles are taken into account ($\Delta E_{\text{spectrometer}} = 550$ meV, $\Delta E_{\text{photon}} = 380$ meV). The solid curve is calculated for $C(4d)$, i.e., it takes into account the PCI induced interference effects between the $4d_{5/2}$ and $4d_{3/2}$ photoionization and accompanied Auger decay channels. Without this interference the curve below 97 eV photon energy is approximately 15% higher; above 98 eV there is no effect since there the amplitude for $C(4d_{5/2})$ coincidences vanishes. From Fig. 2 it can be seen that the experimental data are well described by the solid curve. This confirms the theoretical treatment—in particular, the two basic features of PCI for the selected energy relation $\epsilon_a = \epsilon_b = (\epsilon_P^0 + \epsilon_A^0)/2$: (a) The maximum of the asymmetric intensity profile is shifted towards lower values as compared to the “on-resonance” photon energy $h\nu^0 = 97.52$ eV. (b) Remarkable coincident intensity is observed for rather large energy detunings (compare the solid and dashed curve at about 95.5 eV photon energy).

In summary, we have successfully demonstrated the validity of the proposed PCI description in sequential

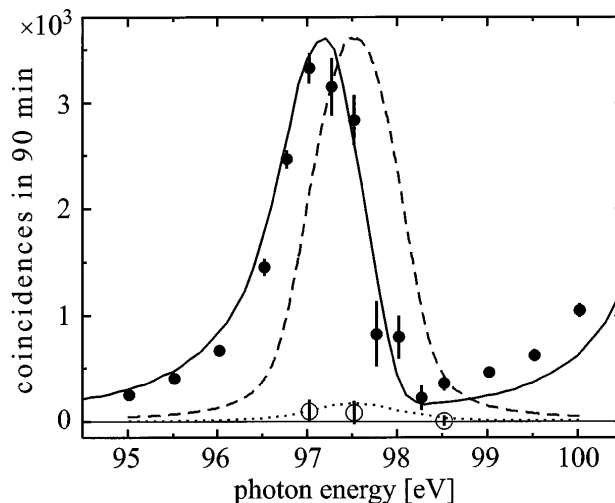


FIG. 2. Photon energy dependence of coincidences between “photo”-electrons and “Auger” electrons in xenon at small relative angles, $\Phi_{a,b} = 20^\circ \pm 4^\circ$, and for electron energies $\epsilon_a = \epsilon_b = (\epsilon_P^0 + \epsilon_A^0)/2$. Experimental data for true $C_{\text{true}}(4d)$ coincidences are given by full circles with error bars. Their zero level is shown by the open circles and the dotted curve. Theoretically predicted data: solid curve for PCI effects included; dashed curve for PCI effects neglected; both curves contain the finite energy resolution and acceptance angles as given in the experiment.

double photoionization for a particular case, small relative angles, and condition for full coherence. Concerning the last point we would like to point out that the present study yields only relative coincidence rates. Therefore, it cannot provide information about the influence which the full coherence has on the observed signal. From the theoretical calculation it follows for the present example that the high degree of symmetry in the experimental parameters ($\Phi_a = -\Phi_b$, $\epsilon_a = \epsilon_b$) gives an increase of the coincidence signal by a factor of 2 as compared to a fully incoherent treatment, i.e., the interference is constructive.

Having control on the setup for measuring coincident electrons at small relative angles in one electron spectrometer, we will replace in a next step the two channeltrons by two position-sensitive, i.e., energy selective detectors, and attempt to measure PCI affected coincident energy distributions for other conditions of coherence/incoherence. The study of interference structures in the coincident energy distributions as well as of the angle-dependent transition probability with its reduction due to PCI will then provide further detailed insight into the fundamental Coulomb interaction between three charged particles which are subject to PCI.

We extend sincere thanks to the members of BESSY, in particular to W. Braun and O. Schwarzkopf for excellent research facilities and to T. Åberg, W. Ketterle, and

W. Schleich for fruitful discussions in which the analogy to quantum optical experiments became clear, and to the financial support through the Deutsche Forschungsgemeinschaft in the SFB 276 TP B5.

-
- [1] T. Åberg, *Phys. Scr.* **21**, 495 (1980); T. Åberg and G. Howat, *Corpuscles and Radiation in Matter: Theory of the Auger Effect*, Encyclopedia of Physics Vol. 31, edited by W. Mehlhorn (Springer, Berlin, 1982), p. 469.
 - [2] L. Végh and J. H. Macek, *Phys. Rev. A* **50**, 4031 (1994).
 - [3] S. A. Sheinerman and V. Schmidt, *J. Phys. B* **30**, 1677 (1997).
 - [4] S. Haroche, M. Brune, J. M. Raimond, E. Hagley, C. Wunderlich, A. Maali, J. Dreger, and X. Maitre, in *Atomic Physics 15: Proceedings of the 15th International Conference on Atomic Physics, Amsterdam, 1996* (World Scientific, Singapore, 1997), p. 1.
 - [5] M. Yu. Kuchiev and S. A. Sheinerman, *Sov. Phys. Usp.* **32**, 569 (1989).
 - [6] M. Yu. Kuchiev and S. A. Sheinerman, *J. Phys. B* **27**, 2943 (1994).
 - [7] W. R. Johnson and K. T. Cheng, *Phys. Rev. A* **46**, 2952 (1992).
 - [8] O. Schwarzkopf and V. Schmidt, *J. Phys. B* **28**, 2847 (1995).